Magnetically Induced Quadrupole Interactions in $FeCr_2S_4$†

GILBERT R. HOY AND K. P. SINGH
Department of Physics, Boston University, Boston, Massachusetts

(Received 22 December 1967)

The effective-field parameters at Fe^{57} nuclei in the cubic normal spinel $FeCr_2S_4$ have been investigated in the temperature range from 60 to 298°K, using the Mössbauer effect. A nonzero quadrupole interaction appears below the effective-magnetic-field transition temperature ($\approx$172°K). The values of the effective internal magnetic field H, the electric field gradient, and the relative orientation of **H** with respect to the principal axes of the electric-field-gradient tensor (EFG) are determined as a function of temperature; e.g., at 77°K, $H=202$ kG, $\frac{1}{2}e^2qQ=-0.62$ mm/sec, and the asymmetry parameter $\eta=0.4$. Predictions based on the theory of a magnetically induced quadrupole interaction do not explain the observed spectra. Assuming $H\propto(1-T/T_N)^\beta$ near the critical point, $\beta=\frac{1}{3}$ gives a better fit to the experimental data than $\beta=\frac{1}{2}$.

I. INTRODUCTION

QUITE a bit of interest has recently been generated by the observation in cubic materials of a nonzero quadrupole interaction arising from magnetic effects. Briefly, the situation is as follows. The effective fields, i.e., electric field gradient and magnetic field at the Fe^{57} nucleus in a ferrous ion as detected by the Mössbauer effect, are primarily determined by the spatial and spin distributions of the electrons in the ion itself. If there is no effective magnetic field at the nucleus and the site symmetry of the ferrous ion is cubic, it follows from symmetry arguments that the electric field gradient will also be zero. However, if the ion is in a magnetic field, either an effective or "real" magnetic field, the electrons' spatial distribution will be altered. Thus even though the ligand symmetry from the position point of view may be cubic, the ferrous ion does not "see" cubic symmetry in this extended sense. The quadrupole interaction due to this effect has been observed. We can divide the observations into two groups: namely, those in which the magnetic field is an effective field due to spontaneous magnetic ordering in the material and those in which the magnetic field is due to an externally applied field. In the first group, experiments have been done in which the divalent Fe^{57} ion was an impurity[1] and in others where it was a natural constituent.[2–6] Very recently experiments have also been done using Fe^{57}- or Co^{57}-doped single crystals of MgO in an external magnetic field.[7,8] These latter experiments seem to demonstrate this effect conclusively. However, the experiments on ferrous compounds below their ordering temperatures, as in the cases of $RbFeF_3$ [2,4] and $FeCr_2S_4$,[3,5,6] have not been so conclusive. For example, in the study of $RbFeF_3$ it was assumed that the ferrous-ion site retained its octahedral ligand symmetry below the transition temperature (T_N = 102°K [2]). However, recent results by Testardi *et al.*[9] show that there is a tetragonal distortion in the region between 101 and 86°K. In the case of $FeCr_2S_4$, neutron diffraction studies[10] indicate that the crystal is cubic down to 4.2°K, which is well below the published transition temperature (T_N = 180°K [10] or 195°K [11]).

In this paper we review the theory using a straightforward model of the magnetically induced quadrupole interaction and test it in the case of $FeCr_2S_4$. In order to do this we have obtained Mössbauer spectra at a number of temperatures between room temperature and 60°K. The effective internal magnetic field and electric-field-gradient parameters are determined at each temperature as is the relative orientation of the internal magnetic field with respect to the principal axes of the electric-field-gradient tensor. These extracted parameters are compared with those predicted by the theory. Various other aspects of our results are pointed out in the appropriate sections below.

II. THEORETICAL REVIEW

The problem of a magnetically (or exchange-field) induced quadrupole interaction has been treated by several authors.[2,4,5,12] In this section we present only a summary of the results. However, since the above references mainly quote results also, we include a fairly detailed and straightforward account in the Appendices.

The two types of symmetries studied are the octahedral Fe^{2+} site in, for example, undistorted $RbFeF_3$ and the tetrahedral site in $FeCr_2S_4$. For the octahedral case (see Appendix A for details), if the magnetic

† Supported by the U.S. Army Research Office, Durham, N.C.

[1] J. D. Siegworth, Phys. Rev. **155**, 285 (1967).
[2] G. K. Wertheim, H. J. Guggenheim, H. J. Williams, and D. N. E. Buchanan, Phys. Rev. **158**, 446 (1967).
[3] G. R. Hoy and S. Chandra, J. Chem. Phys. **47**, 961 (1967).
[4] U. Ganiel, M. Kestigian, and S. Shtrikman, Phys. Letters **24A**, 577 (1967).
[5] M. Eibschutz, S. Shtrikman, and Y. Tenenbaum, Phys. Letters **24A**, 563 (1967).
[6] G. R. Hoy, K. P. Singh, and S. Chandra, in Proceedings of the International Conference on Hyperfine Interactions Detected by Nuclear Radiation, Pacific Grove, Calif., 1967 (unpublished).
[7] J. Chappert, R. B. Frankel, and N. Blum, Bull. Am. Phys. Soc. **12**, 352 (1967).
[8] H. R. Leider and D. N. Pipkorn, Phys. Rev. **165**, 494 (1968).
[9] L. R. Testardi, H. J. Levinstein, and H. J. Guggenheim, Phys. Rev. Letters **19**, 503 (1967).
[10] G. Shirane, D.E. Cox, and S. J. Pickart, J. Appl. Phys. **35**, 954 (1964).
[11] F. K. Lotgering, Philips Res. Rept. **11**, 190 (1956).
[12] F. S. Ham, Phys. Rev. **160**, 328 (1967).

TABLE I. Effective-field parameters in $FeCr_2S_4$.[a]

Absorber temperature (°K)	Magnetic field[b] (kG)	ΔE_Q[c] (mm/sec)	$\frac{1}{2}e^2qQ$ (mm/sec)	η[d]	Γ[e] (mm/sec)
61.0±0.5	203	0.68	−0.64	0.8	0.50
76.6±0.5	199	0.65	−0.62	0.5	0.44
78	202	0.64	−0.62	0.4	0.40
106±1	193	0.53	−0.52	0.1	0.34
121±2	184	0.42	−0.42	0	0.35
130±2	176	0.33	−0.33	0	0.38
139±1	163	0.23	−0.23	0	0.34
148±4	148	0.18	−0.18	0	0.42
154±1	137	0.13	−0.13	0	0.37
161±1	111	0.08	−0.08	0	0.43
163±1	102	0.07	−0.07	0	0.49, 0.35[f]
167±1	79	0.04	−0.04	0	0.61, 0.40, 0.32
168±1	75	0.03	−0.03	0	0.80, 0.46, 0.27
170±1	60	...	...	0	0.67, 0.51, 0.30

[a] These results should be compared with earlier work, Ref. 3.
[b] We estimate a precision of ±2 kG.
[c] We estimate a precision of ±0.02 mm/sec.
[d] We estimate a precision of ±0.1.
[e] The linewidth Γ was determined from least-squares analysis.
[f] At this temperature and above, the spectra could not be fitted using a single linewidth but could be fitted by using equal linewidths for pairs. The first number corresponds to the outermost pair and so on.

field is in the [100] direction, the induced electric-field-gradient parameter $\frac{1}{2}e^2qQ$ is negative. However, if the magnetic field is in the [111] direction, this same parameter is positive. In either case, the asymmetry parameter η is zero and the z axis of the electric-field-gradient tensor (EFG) is collinear with the direction of the magnetic field. The low-temperature value of the quadrupole splitting should be $\Delta E_Q = |\frac{1}{2}e^2qQ| \approx 0.15$ mm/sec, i.e., about 1/20 of the value produced by a single $3d$ orbital electron. For the tetrahedral case (see Appendix B), if the magnetic field is along the [100] direction, $\frac{1}{2}e^2qQ$ is positive, $\eta=0$, and again the z axis of the EFG is along the magnetic field. It appears to be possible to obtain the full single-orbital-level electric field gradient at sufficiently low temperatures ($T<20$°K) in this case. On the other hand, if the magnetic field is along the [111] direction, the electric field gradient should not appear.

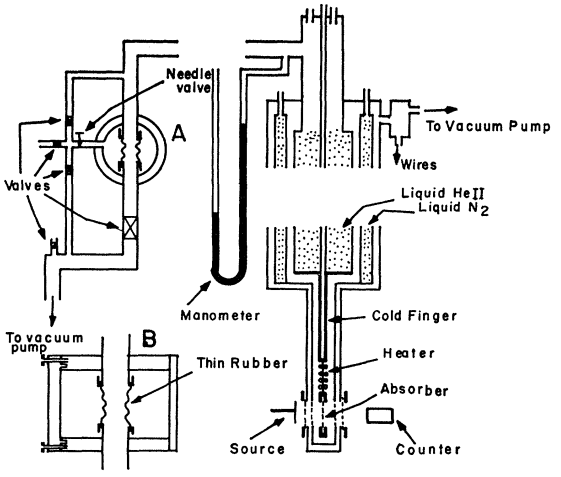

FIG. 1. Liquid-helium Dewar together with pressure regulator system. A and B are two perpendicular cross sections of the pressure regulator system.

III. EXPERIMENTAL SPECTRA AND EFFECTIVE-FIELD PARAMETERS

Our Mössbauer spectrometer system is of conventional design, utilizing a Nuclear Data 512-channel

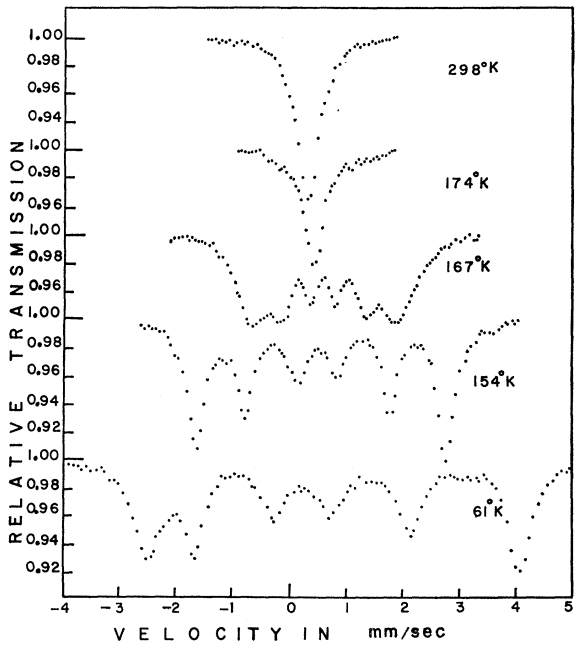

FIG. 2. Mössbauer spectra of powdered $FeCr_2S_4$ as a function of temperature. The spectra are shown on the same velocity scale. A complete list of the effective-field parameters as extracted from such spectra is given in Table I.

TABLE II. Showing **H** is perpendicular to the z axes of the EFG.

Absorber Temperature (°K)	E_1+E_3 (mm/sec)	$2E_2$ (mm/sec)	Deviation $\lvert 2E_2-E_1-E_3 \rvert$	% Deviation	% Linearity[a]
61.0±0.5	2.754	2.808	0.054	1.9	0.4
76.6±0.5	2.710	2.782	0.072	2.6	0.4
78	2.734	2.816	0.082	2.9	0.5
106±1	2.602	2.676	0.074	2.7	0.4
121±2	2.465	2.544	0.079	3.1	0.4
130±2	2.364	2.406	0.042	1.7	0.4
139±1	2.187	2.219	0.032	1.4	0.5
148±4	2.007	1.998	0.009	0.5	0.4
154±1	1.854	1.834	0.020	1.1	0.7
161±1	1.517	1.480	0.037	2.4	0.5
163±1	1.385	1.460	0.025	1.8	0.5
167±1	1.086	1.034	0.052	4.8	0.5
168±1	1.036	0.991	0.045	4.3	0.5

[a] The linearity was estimated by analyzing iron-foil spectra.

analyzer operating in the multichannel scaling mode. The Mössbauer spectra were recorded keeping the absorber fixed and moving the source. The single-line Co^{57}-in-copper source was kept at room temperature at all times. The absorber ($\approx$10 mg/cm^2 of iron) was made by spreading well-powdered $FeCr_2S_4$ uniformly in a Lucite cap of 3/8 in. i.d. which was then pressed by a Lucite disk. The absorber was then mounted in a liquid-helium Dewar (Andonian Associates, Inc.). The details are shown in Fig. 1. For absorber temperatures above liquid nitrogen, a small heater mounted above the absorber on the cold finger was used. The temperatures were regulated to within 1°K with the help of a current control unit. All temperatures were measured using a copper-constantan thermocouple.

The temperatures below liquid-nitrogen temperature were obtained by pumping on the nitrogen vapor. The temperature was regulated to within 1°K by regulating the nitrogen vapor pressure above the liquid nitrogen. Two sections, A and B, of the pressure regulating system are shown in Fig. 1. The pressures were measured using a mercury manometer.

The linearity and gain corresponding to each experimental run were determined by measuring the Doppler spectrum of Fe^{57} in iron foil and sodium nitroprusside. The linearity is better than 1% in all our experiments

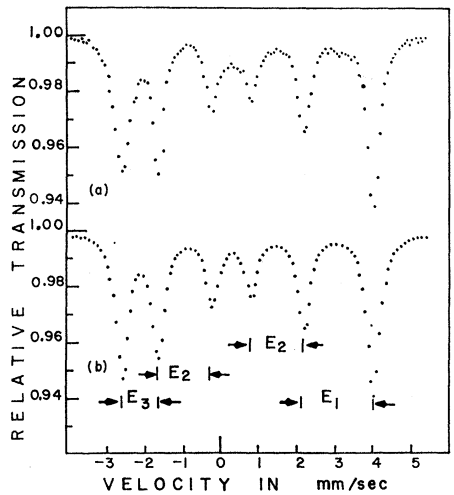

FIG. 3. (a) Normalized Mössbauer spectrum of powdered $FeCr_2S_4$ at liquid-nitrogen temperature; (b) the Lorentzian least-squares fit of the spectrum assuming six lines of equal width. The quantities E_1, E_2, and E_3 are energy spacings between various lines as shown.

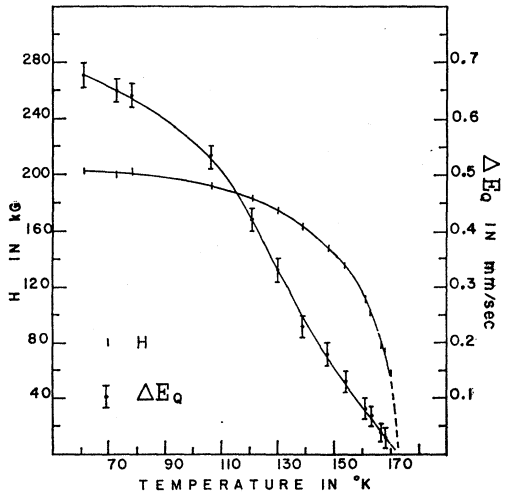

FIG. 4. The temperature dependences of the effective magnetic field (H) and the electric quadrupole interaction (ΔE_Q). Notice that both curves extrapolate to zero at the same temperature (172°K). The lines are just sketched through the experimental points.

as determined by considering the relative separations of the six absorption lines in the iron-foil spectra.

A representative set of Mössbauer spectra for $FeCr_2S_4$ at various temperatures is shown on the same velocity scale in Fig. 2.

In order to extract the effective-field parameters, a Lorentzian least-squares analysis was performed on each $FeCr_2S_4$ Mössbauer spectrum to determine the locations of the absorption peaks. These locations were then used to obtain the effective-field parameters following the technique of Johnson[13] and Hoy and Chandra.[3,14] It is of importance to note that these techniques can be used to determine whether or not the effective internal magnetic field is along one of the principal axes of the EFG. The only experimental information needed is the energy spacings between the Mössbauer peaks. The reason this is possible is that the form of the Hamiltonian, describing the interaction of the nucleus with a magnetic field **H** and an electric field gradient, is the same whenever **H** is along one of the principal axes of the EFG except for a trivial relabeling of axes. Thus, by measuring the Mössbauer peak separations and using the appropriate equations,[13,14] the following information can be obtained: the value of the internal magnetic field; whether or not **H** is along a principal axis of the EFG; if **H** is along a principal axis, whether or not that axis is the z axis; the value of $\frac{1}{2}e^2qQ$; and the value of η. We have made this analysis for all our experimental spectra. Table I summarizes our results for the effective-field parameters. Using the above technique, we determined that the effective internal magnetic field **H** is along a principal axis of the EFG, but not the z axis—i.e., **H** is perpendicular to the z axis.

IV. RESULTS AND CONCLUSIONS

In Fig. 3 we show our experimental data for $FeCr_2S_4$ at liquid-nitrogen temperature. We also show a Lorentzian least-squares fit to our experimental data assuming six lines of equal width. The following question then presents itself: Can we fit spectra such as shown in Fig. 3, assuming $\eta=0$ and an effective magnetic field **H** along the z axis of the EFG? If we were to plot the best values consistent with $\eta=0$ and **H** along the z axis of the EFG, the comparison of these spectra with the experimental result would not show a dramatic difference. However, the suitability of the parameters given in Table I is best demonstrated by the results shown in Table II. If the effective magnetic field is along the z axis of the EFG and $\eta=0$, it is not difficult to show that the quantities $2E_2$ and E_1+E_3, as defined in Fig. 3, must be equal. In Table II we compute the deviations from equality for all our least-squares-analyzed experimental spectra. After considering our experimental linearity, we conclude that these deviations are outside that expected from nonlinearities in our Mössbauer spectrometer.

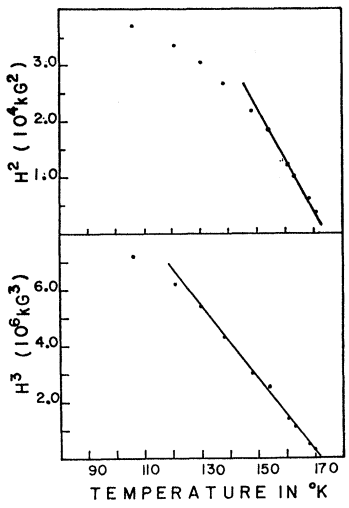

FIG. 5. The measured effective magnetic field quantities H^3 and H^2 are plotted as a function of temperature. The data points corresponding to H^3 give a better straight line. The transition temperature is 172°K.

It is of some interest to estimate the uncertainty in the 90° angle between **H** and the z axis of the EFG. This is especially true since the EFG could arise from two contributions; namely, the theoretically predicted, magnetically induced part and a temperature-dependent lattice distortion contribution. In order to determine the uncertainty in the angle, we tested the quantities E_1, E_3, and E_1+E_3 as a function of the angle between **H** and z using the values of the effective-field parameters in Table I. These quantities were then compared with our experimental values including our estimated experimental linearity. The results are as follows: For those runs at 154°K and below, the error in the angle in question is less than $\pm10°$; for those runs at higher temperatures, the error is larger, perhaps of the order of $\pm20°$. The reason the accuracy in the angle decreases as the temperature increases is that the ratio $R=e^2qQ/\mu H$ is decreasing. The test used to determine that **H** is along a principal axis of the EFG depends on R. When $\eta=0$ and $R\ll1$, first-order perturbation theory is valid and the test fails. From the test shown in Table II and our estimate of the uncertainty in the 90° angle, we conclude that the theoretically predicted, magnetically induced quadrupole interaction is insufficient, by itself, to explain our results.

Having convinced ourselves that the effective-field parameters given in Table I are the correct ones, we show in Fig. 4 the temperature dependence of the effective magnetic field H and the quadrupole interaction ΔE_Q.

[13] C. E. Johnson, Proc. Phys. Soc. (London) **88**, 943 (1966).
[14] S. Chandra, Ph.D. thesis, Boston University, 1967 (unpublished).

If we assume that H is proportional to $[1-(T/T_N)]^\beta$ near the transition temperature, our results shown in Fig. 5 are more consistent with a critical exponent $\beta=\frac{1}{3}$ as compared to $\beta=\frac{1}{2}$. We also obtain a transition temperature of $T_N=172°$K which is in reasonable agreement with the latest measurement.[10]

To summarize, it seems evident that the quadrupole interaction is primarily due to a temperature-dependent lattice distortion associated with magnetostrictive effects. We see from Fig. 4 that both interactions occur below 172°K and grow in strength together. Apparently the neutron diffraction work was not sufficiently exact to observe this effect and we must wait for x-ray studies of single crystals of $FeCr_2S_4$ as in the case of $RbFeF_3$.[9] It seems unlikely that a dynamical Jahn–Teller effect[15] would occur coincidentally at the transition temperature.

ACKNOWLEDGMENTS

We would like to express our deep appreciation to Dr. G. Haacke for sending us samples of $FeCr_2S_4$ and to Dr. G. K. Wertheim for a helpful communication.

APPENDIX A

In this Appendix we present a simple model to explain the magnetically induced quadrupole interaction produced at the nuclei of Fe^{2+} ions in sites of octahedral symmetry. We assume we are dealing with a high-spin case such that the free-ion level $^5D_4$ is split by the cubic field into a low-lying orbital triplet $^5T_{2g}$ and an orbital doublet ^5E_g approximately 20 000 cm^{-1} higher. We completely neglect the effects of the upper orbital doublet. We now suppose that a magnetic field appears at the ion and include also the effects of spin-orbit coupling. The consequences can be handled nicely by making use of the $t_{2g}-p$ equivalence of the orbital triplet level. Following Abragam and Pryce[16] we can introduce an effective angular momentum $L'=1$ for the T_{2g} orbitals. We can then construct an effective total angular momentum $J=L'+S$, where $S=2$. The effect of spin-orbit coupling is to remove the 15-fold total degeneracy and produce a 7-fold level corresponding to $J=3$, a 5-fold level corresponding to $J=2$, and a lowest-lying 3-fold level corresponding to $J=1$. If the strength of the effective magnetic field is sufficiently weak, the eigenstates can be represented by the symbol $|JJ_z\rangle$. Thus the eigenstates corresponding to the lowest-lying spin-orbit levels in the presence of a weak magnetic field can be labeled $|11\rangle$, $|10\rangle$, and $|1\text{-}1\rangle$. Since we are interested in evaluating the electric field gradient produced by the orbital part of the ion at its nucleus, it is convenient to express the eigenstates in the uncoupled representation denoted by $|SS_zL'L'_z\rangle$. This is easily done by evaluating the appropriate Clebsch–Gordan coefficients. The results are[2]

$$\begin{aligned}|11\rangle&=(1/10)^{1/2}|2011\rangle-(3/10)^{1/2}|2110\rangle\\&\quad+(6/10)^{1/2}|221\text{-}1\rangle,\\|10\rangle&=(3/10)^{1/2}|2\text{-}111\rangle-(4/10)^{1/2}|2010\rangle\\&\quad+(3/10)^{1/2}|211\text{-}1\rangle,\\|1\text{-}1\rangle&=(1/10)^{1/2}|201\text{-}1\rangle-(3/10)^{1/2}|2\text{-}110\rangle\\&\quad+(6/10)^{1/2}|2\text{-}211\rangle.\end{aligned}\tag{A1}$$

In order to obtain the field gradient at the nucleus due to the ion, we need to compute $\langle JJ_z|q|JJ_z\rangle$ and $\langle JJ_z|q\eta|JJ_z\rangle$, where q and η are the standard electric-field-gradient parameters.[17] Using the technique of Hoy and Barros,[18] we can write

$$\langle JJ_z|q|JJ_z\rangle=-\langle r^{-3}\rangle_{3d}(16\pi/5)^{1/2}\langle JJ_z|Y_2^0|JJ_z\rangle.\tag{A2}$$

If we write the right-hand side of Eq. (A2) in terms of the uncoupled representation, considering, for example, the state $|JJ_z\rangle=|11\rangle$, we have

$$\langle 11|q|11\rangle=-\langle r^{-3}\rangle_{3d}(16\pi/5)^{1/2}[(1/10)\langle 11|Y_2^0|11\rangle+(3/10)\langle 10|Y_2^0|10\rangle+(6/10)\langle 1\text{-}1|Y_2^0|1\text{-}1\rangle].\tag{A3}$$

Note that the matrix elements on the right-hand side deal with states labeled by $|L'L'_z\rangle$. It is at this point that we see the effect of different orientations of the effective internal magnetic field. The orbital functions must be chosen to be eigenstates of rotations about the axis determined by the magnetic field. In general we must also consider matrix elements of $q\eta$:

$$\langle JJ_z|q\eta|JJ_z\rangle=-\langle r^{-3}\rangle_{3d}3(8\pi/15)^{1/2}\times\langle JJ_z|Y_2^2+Y_2^{-2}|JJ_z\rangle.\tag{A4}$$

It is of some interest to consider particular directions for the effective internal magnetic field. Suppose this direction is [100]. From Ballhausen[19] we can obtain the orbital functions $|L'L'_z\rangle$ quantized along the four-fold [100] axis, namely,

$$\begin{aligned}|11\rangle&=Y_2^{-1},\\|10\rangle&=1/\sqrt{2}(Y_2^2-Y_2^{-2}),\\|1\text{-}1\rangle&=-Y_2^1.\end{aligned}\tag{A5}$$

Thus, for example, Eq. (A3) becomes, using the nota-

[15] W. Moffett and A. D. Liehr, Phys. Rev. **106**, 1195 (1957).
[16] A. Abragam and M. H. Pryce, Proc. Roy. Soc. (London) **A205**, 135 (1951).
[17] G. K. Wertheim, *Mössbauer Effect* (Academic Press Inc., New York, 1964).
[18] G. R. Hoy and F. de S. Barros, Phys. Rev. **139**, A929 (1965).
[19] C. J. Ballhausen, *Ligand Field Theory* (McGraw-Hill Book Company, New York, 1962).

tion of Ref. 18,

$$\langle 11 \mid q \mid 11\rangle = -\langle r^{-3}\rangle_{3d}(16\pi/5)^{1/2}(1/10) \times (G_{20}{}^{-1-1}+3G_{20}{}^{00}+6G_{20}{}^{11}).$$

The results for the $\mid JJ_z\rangle$ states are[2]

$$\langle 11 \mid q \mid 11\rangle = -(1/20)[(4/7)\langle r^{-3}\rangle_{3d}],$$
$$\langle 1\text{-}1 \mid q \mid 1\text{-}1\rangle = -(1/20)[(4/7)\langle r^{-3}\rangle_{3d}],$$
$$\langle 10 \mid q \mid 10\rangle = (1/10)[(4/7)\langle r^{-3}\rangle_{3d}]. \quad \text{(A6)}$$

The value of $\langle JJ_z \mid q\eta \mid JJ_z\rangle$ is zero for all J_z.

Now consider the situation in which the internal magnetic field is in the [111] direction. The proper orbital functions $\mid L'L'_z\rangle$ in this case are

$$\mid 11\rangle = (2/3)^{1/2}Y_2{}^{-2}+(1/3)^{1/2}Y_2{}^{1},$$
$$\mid 10\rangle = Y_2{}^{0},$$
$$\mid 1\text{-}1\rangle = (2/3)^{1/2}Y_2{}^{2}-(1/3)^{1/2}Y_2{}^{1}. \quad \text{(A7)}$$

Using the same procedure as above it is easy to see that $\langle JJ_z \mid q\eta \mid JJ_z\rangle$ is zero for all J_z, and the values of $\langle JJ_z \mid q \mid JJ_z\rangle$ are

$$\langle 11 \mid q \mid 11\rangle = (1/20)[(4/7)\langle r^{-3}\rangle_{3d}],$$
$$\langle 1\text{-}1 \mid q \mid 1\text{-}1\rangle = (1/20)[(4/7)\langle r^{-3}\rangle_{3d}],$$
$$\langle 10 \mid q \mid 10\rangle = -(1/10)[(4/7)\langle r^{-3}\rangle_{3d}]. \quad \text{(A8)}$$

Notice that the signs in Eq. (A8) are opposite from those in Eq. (A6).

In general, the electric field gradient at the nucleus must be determined by a Boltzmann average over the contributing ionic levels. However, it is easily seen that for the case of the magnetic field in the [100] direction the parameter $\frac{1}{2}e^2qQ$ should be negative, and for the [111] direction, $\frac{1}{2}e^2qQ$ should be positive. The magnitude of the quadrupole interaction at sufficiently low temperatures such that only the lowest $\mid JJ_z\rangle$ state is occupied should be $\approx$0.15 mm/sec.

APPENDIX B

In this Appendix we proceed in much the same manner as in Appendix A, but we now suppose the Fe^{2+} sites have tetrahedral symmetry, as in $FeCr_2S_4$. In this case, the twofold orbital level ${}^5E_g$ is lower than the threefold orbital level. This separation is $\Delta\approx$4000 cm^{-1}. The ${}^5E_g$ orbitals transform like states having zero orbital angular momentum, neglecting the upper ${}^5T_{2g}$ levels. Thus, in a first approximation, the levels coming from the ${}^5E_g$ orbitals retain their twofold orbital degeneracy even in the presence of a magnetic field. It is only the spin degeneracy that is removed. It is well known that the electric field gradient at the nucleus due to a double-degenerate E_g orbital is zero. In order to remove this orbital degeneracy, and hence possibly produce an electric field gradient at the nucleus, Eibschutz *et al.*[5] considered the effects of second-order spin-orbit coupling allowing interactions with the upper T_{2g} orbitals. The results are as follows: For a magnetic field in the [100] direction, the orbital degeneracy is removed and the two E_g orbitals are split by an amount $12\lambda^2/\Delta\approx$20°K. The lower orbital level is predominantly $1/\sqrt{2}\mid Y_2{}^2+Y_2{}^{-2}\rangle$, corresponding to a positive electric-field-gradient parameter e^2qQ. The major axis of the EFG is in the [100] direction and the asymmetry parameter is zero.

If the effective magnetic field is along the [111] direction, the orbital degeneracy is not removed and thus no electric field gradient should be produced at the nucleus.